

A TOOL FOR THE AUTOMATIC MODELING OF CAPACITIVE MEMS GYROSCOPES

F. Mair¹, M. Egretzberger¹, A. Kugi¹

¹ Vienna University of Technology, Austria

Corresponding author: F. Mair, Vienna University of Technology, Automation and Control Institute,
Gußhausstraße 27-29, 1040 Vienna, Austria, mair@acin.tuwien.ac.at

Abstract. This paper presents a tool to automatically generate the mathematical model of capacitive MEMS gyroscopes in a symbolic form from geometric input data. The resulting equations can be used for further analysis and controller design within the computer algebra program *Maple* [7]. Additionally, a *Level 2 C-Code S-Function* code generator provides a link to the well known numeric simulation environment MATLAB/Simulink [8].

1 Introduction

Since Micro-Electro-Mechanical-Systems (MEMS) are complex devices, the systematic derivation of an appropriate mathematical model is a challenging task. In general, MEMS comprise components or sub-systems from different physical domains like rigid and elastic mechanical structures, capacitors, inductors, optical and fluidic elements. Therefore, one has to deal with the adequate laws of continuum mechanics, electromagnetism and thermodynamics in order to derive a suitable mathematical formulation.

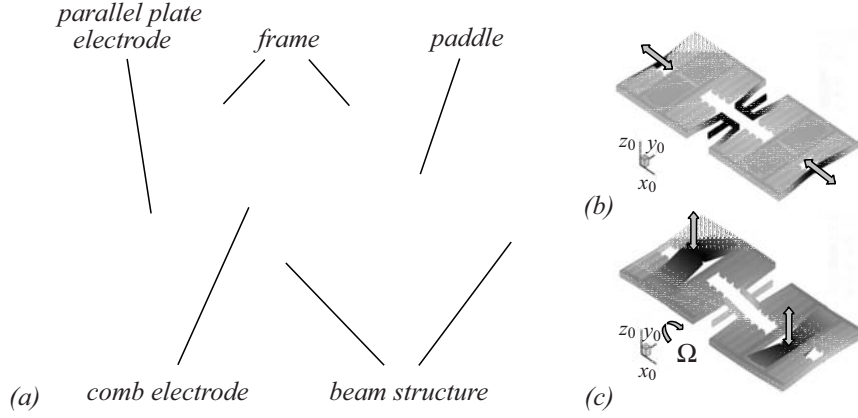
The demands on the mathematical models vary strongly with the intended applications. In order to understand the basic mode of operation, typically lumped parameter models are used, which in general are insufficient in terms of accuracy. By means of the Finite Element Method (FEM) on the other hand it is possible to reproduce the dynamic behavior at a high level of detail, even if the geometry of the device is complex. Therefore, such models are used in a broad range of applications such as the analysis of elastic mechanical structures (e.g., the calculation of eigenfrequencies, stress or strain distributions), the determination of thermodynamical interactions, the calculation of electrostatic and electromagnetic fields, etc. This method, however, has the disadvantage that the resulting system of differential equations is very large and therefore can neither be used for the controller design nor for transient simulations within reasonable time. For this reason, considerable research activities have been conducted in the field of model order reduction techniques, see, e.g., [6], [11], [12] with application to MEMS. Thereby, lower order systems are derived still representing the essential dynamic behavior of the large scale finite element models with sufficient accuracy. The drawback of these techniques is that the systematic order reduction of non-linear systems, which we have to deal with when modeling capacitive actuators and sensors, is still an open issue. An alternative approach to receive a mathematical description with a reasonable number of state variables is to partition the device into functional components (e.g., rigid bodies, elastic bodies, lumped capacitors, etc.) before deriving the actual mathematical representation.

Although there are several commercially available simulation environments (e.g., Ansys[1], COMSOL[2], Coventor[3]) which cope with the mathematical modeling of MEMS, none of these tools is capable of extracting a symbolic representation of the device under consideration. In view of this shortcoming, a software is presented in this paper to derive the non-linear mathematical model of capacitive gyroscopes in a symbolic form from the geometry data available from CAD tools.

2 Mathematical concept

In order to specify the functionality of the software, at first the basic mathematical concepts will be explained by means of a demonstrative example. Figure 1 shows a single axis capacitive gyroscope [5] which is designed to measure the externally applied angular rate signal Ω by means of the *Coriolis effect*. As illustrated in Figure 1 (a), the device is composed of several individual elements, i.e., the movable mechanical structure consisting of rigid elements (frame, paddle) and elastic elements (beam structures), and the fixed electrodes (comb electrodes and parallel plate electrodes). The emerging gaps between the fixed electrodes and the movable structure are forming capacitors, which in turn can be utilized as capacitive actuators and sensors. A harmonic voltage is applied to the in-plane capacitive comb actuators, exciting the movable structure to oscillate in the x_0 -direction as depicted in Figure 1 (b). If the device is undergoing a rotation about the y_0 -axis due to an external angular rate signal Ω , the *Coriolis force* causes an oscillation of the movable structure in the z_0 -direction as depicted in Figure 1 (c). This oscillation is captured by measuring the capacitance change of the capacitive parallel-plate sensor elements.

In a more general form, the capacitive gyroscope can be considered as a multi-body system composed of rigid bodies and elastic bodies. Figure 2 shows an arbitrary rigid body \mathcal{R}_α , an arbitrary elastic body \mathcal{E}_β and an arbitrary capacitor \mathcal{C}_γ to illustrate the following considerations. Let us introduce a spatial reference system $(o_0x_0y_0z_0)$ and material coordinate systems $(o_\alpha x_\alpha y_\alpha z_\alpha)$ and $(o_\beta x_\beta y_\beta z_\beta)$. A rigid body \mathcal{R}_α is characterized by its mass m_α , its


Figure 1: Capacitive gyroscope

inertia tensor \mathbf{J}_α and the center of mass \mathcal{S}_α . According to [13], a rigid body motion is defined by a combination of pure translation and pure rotation why it is reasonable to utilize the translatory degrees-of-freedom $\mathbf{v}_0^\alpha \in \mathbb{R}^3$ and the rotatory degrees-of-freedom $\boldsymbol{\phi}_0^\alpha \in \mathbb{R}^3$, which allow for the parametrization of the rotation $\mathbf{R}_0^\alpha \in SO(3)$, as the generalized coordinates. In order to simplify the notation, the translatory degrees-of-freedom \mathbf{v}_0^α and the rotatory degrees-of-freedom $\boldsymbol{\phi}_0^\alpha$ are merged to a vector of displacements and rotations $\mathbf{r}_0^\alpha = [\mathbf{v}_0^\alpha, \boldsymbol{\phi}_0^\alpha]^\top \in \mathbb{R}^6$.

Now let \mathbf{S}_0^α and $\mathbf{s}_0^\alpha(t)$ denote the position vectors to the center of mass in the undeformed and deformed configuration, respectively. Then the current translation vector of the center of mass reads as $\mathbf{v}_0^\alpha(t) = \dot{\mathbf{s}}_0^\alpha(t) - \dot{\mathbf{S}}_0^\alpha$. If the reference system is subject to a rotation about the y_0 -axis with the angular velocity Ω relative to an inertial system $(o_I x_I y_I z_I)$, the absolute velocity of the center of mass expressed in the reference system is $(\dot{\mathbf{s}}_I^\alpha)_0 = \boldsymbol{\omega}_0^I \times \mathbf{s}_0^\alpha + \dot{\mathbf{s}}_0^\alpha$ with the angular velocity vector $\boldsymbol{\omega}_0^I = [0, \Omega, 0]^\top$. In order to calculate the kinetic energy of the rigid body \mathcal{R}_α it is advantageous to express the angular velocity vector in the material coordinate system $(\boldsymbol{\omega}_I^\alpha)_\alpha = \mathbf{R}_0^\alpha (\boldsymbol{\omega}_0^I + \boldsymbol{\omega}_0^I)$, with the rotation matrix \mathbf{R}_0^α and the associated angular velocity vector $\boldsymbol{\omega}_0^\alpha$, yielding, see, e.g., [13],

$$T_\alpha = \frac{1}{2} m_\alpha (\dot{\mathbf{s}}_I^\alpha)_0^\top (\dot{\mathbf{s}}_I^\alpha)_0 + \frac{1}{2} (\boldsymbol{\omega}_I^\alpha)_\alpha^\top \mathbf{J}_\alpha (\boldsymbol{\omega}_I^\alpha)_\alpha. \quad (1)$$

Since a rigid body has the property that the displacement of an arbitrary point $\mathcal{X}_k \in \mathcal{R}_\alpha$ can be expressed in the form $\mathbf{u}_0^k(\mathbf{X}_0^k, t) = (\mathbf{R}_0^\alpha(\boldsymbol{\phi}_0^\alpha) - \mathbf{I})(\mathbf{X}_0^k - \mathbf{S}_0^\alpha) + \mathbf{v}_0^\alpha(t)$ and $\boldsymbol{\phi}_0^k = \boldsymbol{\phi}_0^\alpha$ with the position vector \mathbf{X}_0^k in the undeformed configuration as depicted in Figure 2, the components of the vector of displacements and rotations $\mathbf{r}_0^k = [\mathbf{u}_0^k, \boldsymbol{\phi}_0^k]^\top \in \mathbb{R}^6$ can be expressed as functions of the generalized coordinates of the associated rigid bodies.

For the further considerations it is assumed that the mass of the elastic bodies is negligible compared to the mass of the rigid bodies and that the overall displacements of the bodies are small. If an elastic body \mathcal{E}_β is connected to w rigid bodies \mathcal{R}_{α_i} , the above assumptions allow for the calculation of the strain energy in the form

$$V_\beta = \frac{1}{2} (\mathbf{r}_0^\beta)^\top \mathbf{K}_0^\beta \mathbf{r}_0^\beta \quad (2)$$

with the stiffness matrix \mathbf{K}_0^β and the vector $\mathbf{r}_0^\beta = [\mathbf{u}_0^{\alpha_1\beta}, \boldsymbol{\phi}_0^{\alpha_1\beta}, \dots, \mathbf{u}_0^{\alpha_w\beta}, \boldsymbol{\phi}_0^{\alpha_w\beta}]^\top \in \mathbb{R}^{6w}$, merging the displacements and rotations at the intersection points $\mathcal{X}_{\alpha_i\beta}$ with the rigid bodies \mathcal{R}_{α_i} , $i = 1, \dots, w$. If the elastic body is rigidly connected to the reference frame at the intersection point \mathcal{X}_0 then the displacements and rotations are vanishing, i.e., $\mathbf{u}_0^0 = \mathbf{0}$, $\boldsymbol{\phi}_0^0 = \mathbf{0}$. Finally, the capacitance C_γ of an electrostatic actuator forming a capacitor \mathcal{C}_γ together with the rigid body \mathcal{R}_α is derived as a function of the vector of displacements and rotations $\mathbf{r}_0^\gamma = [\mathbf{u}_0^{\alpha\gamma}, \boldsymbol{\phi}_0^{\alpha\gamma}]^\top \in \mathbb{R}^6$ at an associated point $\mathcal{X}_{\alpha\gamma}$ on the surface of the rigid body. Then the potential (co-)energy provided by the electrostatic actuator reads as

$$V_\gamma = \frac{1}{2} C_\gamma \mathbf{r}_0^\gamma (U_\gamma)^2 \quad (3)$$

with the applied voltage U_γ .

Now if it is assumed that a rigid body is solely connected to elastic bodies and vice versa and no generalized forces are acting on the system, Lagrange's formalism

$$\frac{d}{dt} \left(\frac{\partial T}{\partial \dot{\mathbf{z}}} \right)^\top - \left(\frac{\partial T}{\partial \mathbf{z}} \right)^\top + \left(\frac{\partial V}{\partial \mathbf{z}} \right)^\top = \mathbf{0} \quad (4)$$

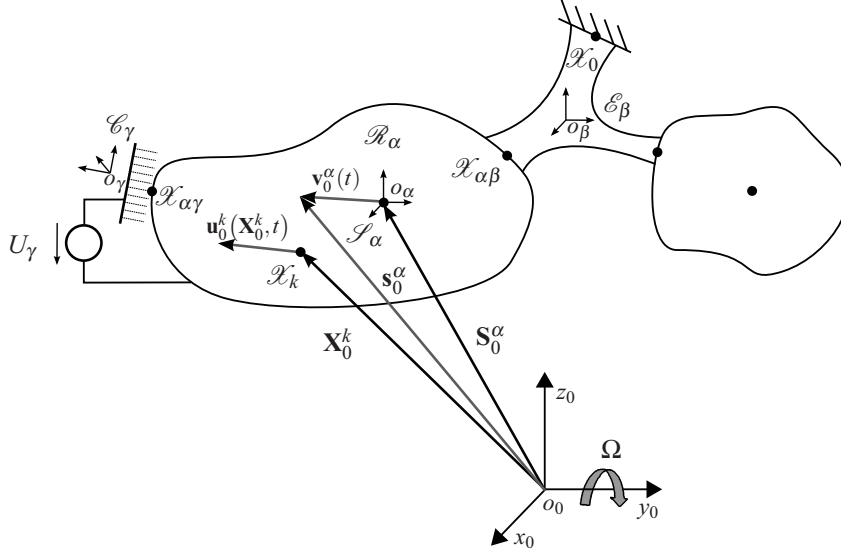


Figure 2: Displacement of bodies

can be applied with the generalized coordinates $\mathbf{z} = [\mathbf{r}_0^{\alpha_1}, \dots, \mathbf{r}_0^{\alpha_n}]^T$ of n rigid bodies, the total kinetic energy $T = \sum_{\alpha} T_{\alpha}$ and the total potential energy $V = \sum_{\beta} V_{\beta} - \sum_{\gamma} V_{\gamma}$.

Referring to [13] equation (4) can be written in the form

$$\mathbf{M}(\mathbf{z})\ddot{\mathbf{z}} + \mathbf{C}(\Omega, \mathbf{z}, \dot{\mathbf{z}})\dot{\mathbf{z}} + \mathbf{f}(\Omega, \dot{\Omega}, \mathbf{z}, \bar{\mathbf{u}}_{\gamma}) = \mathbf{0} \quad (5)$$

with the inertia matrix $\mathbf{M}(\mathbf{z})$, the matrix $\mathbf{C}(\Omega, \mathbf{z}, \dot{\mathbf{z}})$ comprising the centrifugal and Coriolis terms, the vector $\mathbf{f}(\Omega, \dot{\Omega}, \mathbf{z}, \bar{\mathbf{u}}_{\gamma})$ consisting of all terms that result from the potential energy as well as the centrifugal and inertia terms that arise from the external rotation of the reference system with the angular rate Ω . The vector $\bar{\mathbf{u}}_{\gamma}$ consists of the m applied voltages $\bar{\mathbf{u}}_{\gamma} = [U_{\gamma_1}, \dots, U_{\gamma_m}]^T$. The output of the system

$$\mathbf{y} = \mathbf{g}(\mathbf{z}) \quad (6)$$

is given by the vector of capacities $\mathbf{g} = [C_{\gamma_1}, \dots, C_{\gamma_p}]^T$ of the p sense structures.

3 Software

In the following section the developed software for the automatic generation of the mathematical model of capacitive MEMS gyroscopes will be described. Figure 3 illustrates the overall program structure. As it can be seen from the diagram, the software tool is composed of two parts. The first one, *SimMEMS*, is implemented in the object oriented scripting language *Python* [10] and provides the functionality to extract the necessary information from the geometry data to represent the device under consideration with the mathematical representation derived in Section 2. The second part, *ModelMEMS*, is implemented as a library in the commercial computer algebra system *Maple* and provides a symbolic mathematical model of the introduced elements (e.g., rigid bodies \mathcal{R} , elastic bodies \mathcal{E} , capacitors \mathcal{C}).

3.1 SimMEMS

The sensor analysis in *SimMEMS* proceeds in several steps. First, the input file which has to comply with a certain format, is read. This input file consists of different parts describing the material, the geometry and the topology of the device. In the current version, the geometry data is limited to cuboid elements but there are no limitations concerning the number and size of elements defined in the file. As in most cases the geometry data is exported from CAD tools which do not contain any information about the function of the individual geometry elements, several topology algorithms have been implemented to derive the detailed composition of the device. The user only has to provide the information whether a cuboid is part of a rigid or elastic structure or an electrode and the mentioned algorithms ensure that rigid body elements that intersect with other rigid body elements are merged to

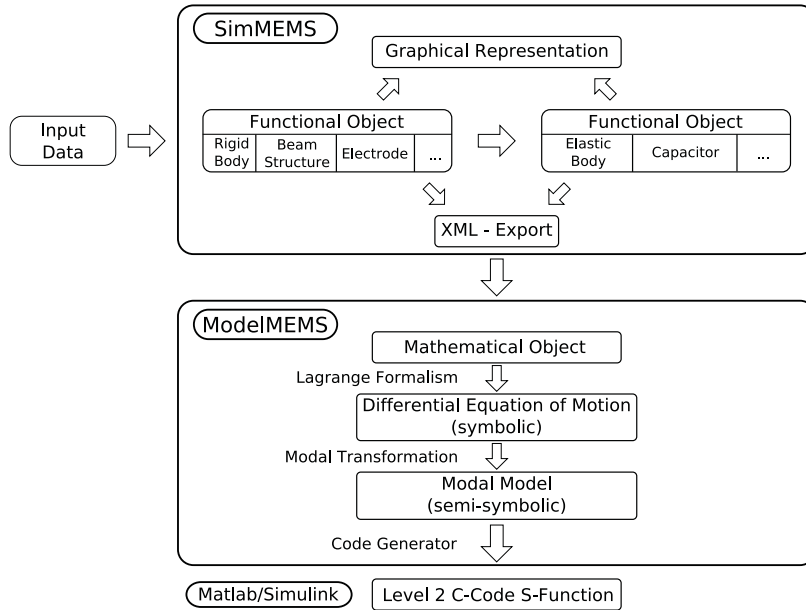


Figure 3: Program structure

one composite rigid body and elastic beam elements that intersect with other elastic beam elements are merged to one composite beam structure.

As a result of the first step, the specific functional components of the sensor (i.e., rigid body, beam structure and electrode) are represented by software classes which will be referred to as functional objects from now on. Based on these functional objects the analysis is continued yielding a further set of functional objects, i.e., elastic body and capacitor. Together, these objects represent the mathematical properties of rigid bodies \mathcal{R} , elastic bodies \mathcal{E} and capacitors \mathcal{C} . To make the following analysis steps comprehensible, all functional objects have a geometrical representation and can be visualized in an integrated 3D viewer. Additionally, to make the program as flexible as possible an interactive interpreter and an editor frame have been added such that all objects can be arbitrarily changed and scripts for reusable tasks can be developed.

Rigid body

Due to the fact that a rigid body \mathcal{R}_α is composed of a set of cuboid elements, its mass m_α , the position vector from the origin of the reference frame to the center of mass \mathbf{S}_0^α in the undeformed configuration and its inertia tensor \mathbf{J}_α with respect to the center of mass can be calculated by means of the well known equations from rigid body dynamics, see, e.g., [13].

Elastic body

The specification of the strain energy (2) of an elastic body is usually more challenging due to various reasons. First, the geometry of such elastic elements can be complicated and an approximation by cuboid elements is usually not sufficiently accurate. Second, as the device is built of the cubic material silicon, the stiffness matrix \mathbf{K}_0^β of a cuboid beam element can just be given symbolically for specific directions of the anisotropic material, see [4]. Therefore, in order to gain the maximal flexibility, the definition of an elastic body object \mathcal{E}_β can be achieved in two ways. The first method is to define it directly in the input file by defining the stiffness matrix \mathbf{K}_0^β , e.g., acquired by means of a finite element analysis and the position vectors $\mathbf{X}_0^{\alpha;\beta}$ in the undeformed configuration of its connection nodes $\mathcal{X}_{\alpha;\beta}$.

The second option is to derive it from a beam structure object. Although this procedure is limited to cuboid beam elements, it is applicable for many sensor designs. In the following, it is assumed that the mass of the elastic beam elements are negligible in comparison to the mass of the rigid bodies and that the overall displacements of the bodies are small. Figure 4 illustrates an individual elastic beam element \mathcal{B}_i . Referring to [9], an elastic beam element, approximated by the Bernoulli-Euler theory, can be described by the relation

$$\begin{bmatrix} \hat{\mathbf{p}}_0^s \\ \hat{\mathbf{p}}_0^e \end{bmatrix} = \underbrace{\begin{bmatrix} \hat{\mathbf{K}}_{ss} & \hat{\mathbf{K}}_{se} \\ \hat{\mathbf{K}}_{es} & \hat{\mathbf{K}}_{ee} \end{bmatrix}}_{\hat{\mathbf{K}}_0^i} \begin{bmatrix} \hat{\mathbf{r}}_0^s \\ \hat{\mathbf{r}}_0^e \end{bmatrix} \quad \text{with} \quad \hat{\mathbf{K}}_{es} = \hat{\mathbf{K}}_{se}^T, \quad (7)$$

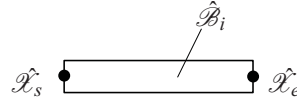


Figure 4: Individual beam element

with the stiffness matrix $\hat{\mathbf{K}}_0^i$, the vectors $\hat{\mathbf{p}}_0^s = [\mathbf{f}_0^s, \mathbf{t}_0^s]^T \in \mathbb{R}^6$, $\hat{\mathbf{p}}_0^e = [\mathbf{f}_0^e, \mathbf{t}_0^e]^T \in \mathbb{R}^6$ containing the forces $\mathbf{f}_0^s, \mathbf{f}_0^e$ and torques $\mathbf{t}_0^s, \mathbf{t}_0^e$ and the vectors $\hat{\mathbf{r}}_0^s = [\mathbf{u}_0^s, \boldsymbol{\phi}_0^s]^T \in \mathbb{R}^6$, $\hat{\mathbf{r}}_0^e = [\mathbf{u}_0^e, \boldsymbol{\phi}_0^e]^T \in \mathbb{R}^6$ consisting of the translational displacements $\mathbf{u}_0^s, \mathbf{u}_0^e$ and rotations $\boldsymbol{\phi}_0^s, \boldsymbol{\phi}_0^e$ at the start $\hat{\mathcal{X}}_s$ and end node $\hat{\mathcal{X}}_e$, all expressed in the spatial reference frame $(o_0x_0y_0z_0)$. If the beam structure object is composed of a single elastic beam element, the potential energy of the resulting elastic body \mathcal{E}_β can be calculated according to (2), with $\mathbf{K}_0^\beta = \hat{\mathbf{K}}_0^i$ and $\mathbf{r}_0^\beta = [\hat{\mathbf{r}}_0^s, \hat{\mathbf{r}}_0^e]^T$. If, however, the beam structure object is composed of several elastic beam elements, further considerations have to be made. To make this more comprehensible, the procedure will be explained by means of an illustrative example. Figure 5 (a) illustrates a T-shaped beam structure with three connection nodes $\mathcal{X}_{\alpha_i\beta}$, $i \in \{1, 2, 3\}$. The elements \mathcal{B}_1 and \mathcal{B}_2 of the beam structure are replaced by suitable elements $\hat{\mathcal{B}}_1$, $\hat{\mathcal{B}}_2$ and $\hat{\mathcal{B}}_3$, as illustrated in Figure 5 (b), that ensure certain required kinematic boundary conditions. Relation (7), given for every beam element $\hat{\mathcal{B}}_i$, allows for assembling a single linear mapping

$$\begin{bmatrix} \hat{\mathbf{p}}_0^1 \\ \hat{\mathbf{p}}_0^2 \\ \hat{\mathbf{p}}_0^3 \\ \hat{\mathbf{p}}_0^4 \\ \hat{\mathbf{p}}_0^5 \\ \hat{\mathbf{p}}_0^6 \end{bmatrix} = \begin{bmatrix} \hat{\mathbf{K}}_{11} & \hat{\mathbf{K}}_{12} & \mathbf{0} & \mathbf{0} & \mathbf{0} & \mathbf{0} \\ \hat{\mathbf{K}}_{21} & \hat{\mathbf{K}}_{22} & \mathbf{0} & \mathbf{0} & \mathbf{0} & \mathbf{0} \\ \mathbf{0} & \mathbf{0} & \hat{\mathbf{K}}_{33} & \hat{\mathbf{K}}_{34} & \mathbf{0} & \mathbf{0} \\ \mathbf{0} & \mathbf{0} & \hat{\mathbf{K}}_{43} & \hat{\mathbf{K}}_{44} & \mathbf{0} & \mathbf{0} \\ \mathbf{0} & \mathbf{0} & \mathbf{0} & \mathbf{0} & \hat{\mathbf{K}}_{55} & \hat{\mathbf{K}}_{56} \\ \mathbf{0} & \mathbf{0} & \mathbf{0} & \mathbf{0} & \hat{\mathbf{K}}_{65} & \hat{\mathbf{K}}_{66} \end{bmatrix} \begin{bmatrix} \hat{\mathbf{r}}_0^1 \\ \hat{\mathbf{r}}_0^2 \\ \hat{\mathbf{r}}_0^3 \\ \hat{\mathbf{r}}_0^4 \\ \hat{\mathbf{r}}_0^5 \\ \hat{\mathbf{r}}_0^6 \end{bmatrix}$$

forming the relation

$$\hat{\mathbf{p}} = \hat{\mathbf{K}}\hat{\mathbf{r}} \tag{8}$$

of the vector of forces and torques $\hat{\mathbf{p}}$ and the vector of displacements and rotations $\hat{\mathbf{r}}$ at the outer nodes $\hat{\mathcal{X}}_{i\beta}$, $i \in \{1, 4, 6\}$ and inner nodes $\hat{\mathcal{X}}_{j\beta}$, $j \in \{2, 3, 5\}$. As it can be seen in Figure 5 (b), the inner nodes $\hat{\mathcal{X}}_{j\beta}$, $j \in \{2, 3, 5\}$ satisfy the kinematic boundary condition $\hat{\mathbf{r}}_0^2 = \hat{\mathbf{r}}_0^3 = \hat{\mathbf{r}}_0^5$. As a consequence, the vector of displacements and rotations $\hat{\mathbf{r}}$ can be expressed by a new vector $\bar{\mathbf{r}} = [\hat{\mathbf{r}}_0^1, \hat{\mathbf{r}}_0^2, \hat{\mathbf{r}}_0^4, \hat{\mathbf{r}}_0^6]^T$ using the singular mapping

$$\hat{\mathbf{r}} = \bar{\mathbf{H}}\bar{\mathbf{r}} \tag{9}$$

with the transformation matrix

$$\bar{\mathbf{H}} = \begin{bmatrix} \mathbf{I} & \mathbf{0} & \mathbf{0} & \mathbf{0} \\ \mathbf{0} & \mathbf{I} & \mathbf{0} & \mathbf{0} \\ \mathbf{0} & \mathbf{I} & \mathbf{0} & \mathbf{0} \\ \mathbf{0} & \mathbf{0} & \mathbf{I} & \mathbf{0} \\ \mathbf{0} & \mathbf{I} & \mathbf{0} & \mathbf{0} \\ \mathbf{0} & \mathbf{0} & \mathbf{0} & \mathbf{I} \end{bmatrix}. \tag{10}$$

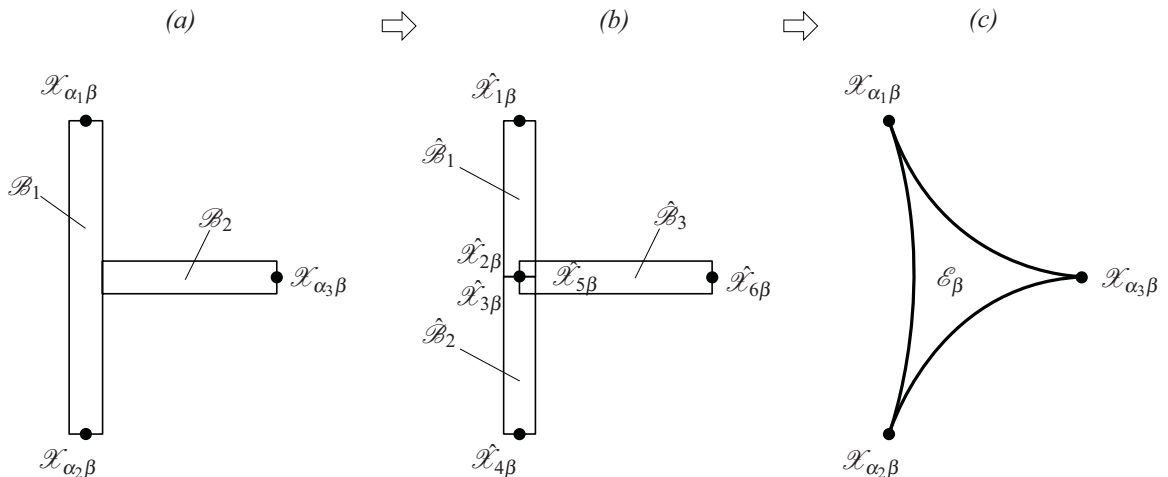


Figure 5: Beam structure to elastic body

Inserting equation (9) into relation (8) and multiplying it with the transpose transformation matrix $\bar{\mathbf{H}}^T$ from the left hand side yields

$$\underbrace{\bar{\mathbf{H}}^T \hat{\mathbf{p}}}_{\bar{\mathbf{p}}} = \underbrace{\bar{\mathbf{H}}^T \hat{\mathbf{K}} \bar{\mathbf{H}}}_{\bar{\mathbf{K}}} \bar{\mathbf{r}}. \quad (11)$$

In the resulting vector of forces and torques $\bar{\mathbf{p}}$ one can see that, according to the static boundary conditions, the sum of forces and torques at the node $\mathcal{X}_{2\beta}$ must be zero, yielding

$$\bar{\mathbf{p}} = \begin{bmatrix} \hat{\mathbf{p}}_0^1 \\ \hat{\mathbf{p}}_0^2 + \hat{\mathbf{p}}_0^3 + \hat{\mathbf{p}}_0^5 \\ \hat{\mathbf{p}}_0^4 \\ \hat{\mathbf{p}}_0^6 \end{bmatrix} = \begin{bmatrix} \hat{\mathbf{p}}_0^1 \\ \mathbf{0} \\ \hat{\mathbf{p}}_0^4 \\ \hat{\mathbf{p}}_0^6 \end{bmatrix}.$$

In order to obtain a re-ordered vector of forces and torques $\tilde{\mathbf{p}}$, in which the zero-entries of all remaining inner nodes (in this example just one) appear in the lower entries, the vector $\bar{\mathbf{p}}$ must be multiplied with the permutation matrix

$$\tilde{\mathbf{H}} = \begin{bmatrix} \mathbf{I} & \mathbf{0} & \mathbf{0} & \mathbf{0} \\ \mathbf{0} & \mathbf{0} & \mathbf{I} & \mathbf{0} \\ \mathbf{0} & \mathbf{0} & \mathbf{0} & \mathbf{I} \\ \mathbf{0} & \mathbf{I} & \mathbf{0} & \mathbf{0} \end{bmatrix}$$

resulting in

$$\tilde{\mathbf{p}} = \tilde{\mathbf{H}} \bar{\mathbf{p}} = \begin{bmatrix} \mathbf{p}_0^\beta \\ \mathbf{0} \end{bmatrix} \quad \text{with} \quad \mathbf{p}_0^\beta = \begin{bmatrix} \hat{\mathbf{p}}_0^1 \\ \hat{\mathbf{p}}_0^4 \\ \hat{\mathbf{p}}_0^6 \end{bmatrix}.$$

A permutation matrix always satisfies $\tilde{\mathbf{H}}^T \tilde{\mathbf{H}} = \tilde{\mathbf{H}} \tilde{\mathbf{H}}^T = \mathbf{I}$. Substituting $\tilde{\mathbf{p}} = \tilde{\mathbf{H}}^T \bar{\mathbf{p}}$ into (11), multiplying with $\tilde{\mathbf{H}}$ and expanding with $\tilde{\mathbf{H}}^T \tilde{\mathbf{H}}$ yields

$$\underbrace{\tilde{\mathbf{H}} \tilde{\mathbf{H}}^T}_{\mathbf{I}} \tilde{\mathbf{p}} = \underbrace{\tilde{\mathbf{H}} \bar{\mathbf{K}} \tilde{\mathbf{H}}^T}_{\tilde{\mathbf{K}}} \underbrace{\tilde{\mathbf{H}} \bar{\mathbf{r}}}_{\tilde{\mathbf{r}}} \quad (12)$$

with the new vector of displacements and rotations

$$\tilde{\mathbf{r}} = \begin{bmatrix} \mathbf{r}_0^\beta \\ \hat{\mathbf{r}}_0^2 \end{bmatrix} \quad \text{with} \quad \mathbf{r}_0^\beta = \begin{bmatrix} \hat{\mathbf{r}}_0^1 \\ \hat{\mathbf{r}}_0^4 \\ \hat{\mathbf{r}}_0^6 \end{bmatrix}.$$

In order to present the further considerations clearer, (12) is written in the form

$$\begin{bmatrix} \mathbf{p}_0^\beta \\ \mathbf{0} \end{bmatrix} = \begin{bmatrix} \tilde{\mathbf{K}}_{\beta\beta} & \tilde{\mathbf{K}}_{\beta 0} \\ \tilde{\mathbf{K}}_{0\beta} & \tilde{\mathbf{K}}_{00} \end{bmatrix} \begin{bmatrix} \mathbf{r}_0^\beta \\ \hat{\mathbf{r}}_0^2 \end{bmatrix}.$$

The vector of displacements and rotations $\hat{\mathbf{r}}_0^2$ at the inner node $\mathcal{X}_{2\beta}$ can now be expressed by the linear mapping

$$\hat{\mathbf{r}}_0^2 = -\tilde{\mathbf{K}}_{00}^{-1} \tilde{\mathbf{K}}_{0\beta} \mathbf{r}_0^\beta$$

of the vector of displacements and rotations \mathbf{r}_0^β at the outer nodes $\mathcal{X}_{i\beta}$, $i \in \{1, 4, 6\}$. Thus, the desired relation finally reads as

$$\mathbf{p}_0^\beta = \underbrace{(\tilde{\mathbf{K}}_{\beta\beta} - \tilde{\mathbf{K}}_{\beta 0} \tilde{\mathbf{K}}_{00}^{-1} \tilde{\mathbf{K}}_{0\beta})}_{\mathbf{K}_0^\beta} \mathbf{r}_0^\beta,$$

with the stiffness matrix \mathbf{K}_0^β , permitting the description of the potential energy of an elastic body \mathcal{E}_β according to (2).

Capacitor

In the last analysis step, the capacitor elements \mathcal{E}_γ are derived. As indicated in Section 2, only capacitor elements emerging between the statically mounted electrodes and the movable rigid bodies are considered. The capacitances depend on the generalized coordinates and can therefore be used as actuators and sensors. Under the assumption that the rigid body \mathcal{R}_α and electrode are parallel in the undeformed configuration, as a result of the geometric structure of the elements under consideration, a capacitor \mathcal{E}_γ is always composed of one or more rectangular plate elements \mathcal{E}_γ^i with constant initial gap distance g_0 and initial rectangular overlap area $A_{\alpha\gamma}^0$, as illustrated in Figure 6. For the further considerations, let us introduce a coordinate system $(o_\gamma x_\gamma y_\gamma z_\gamma)$, whose origin o_γ is located on the bottom side of the electrode, orientated in such way that z_γ is aligned normal to the planar surface of the electrode and x_γ and y_γ are in direction of the lateral edges of the overlap area $A_{\alpha\gamma}^0$. Then, the displacement of a point $\mathcal{X}_{\alpha\gamma}$

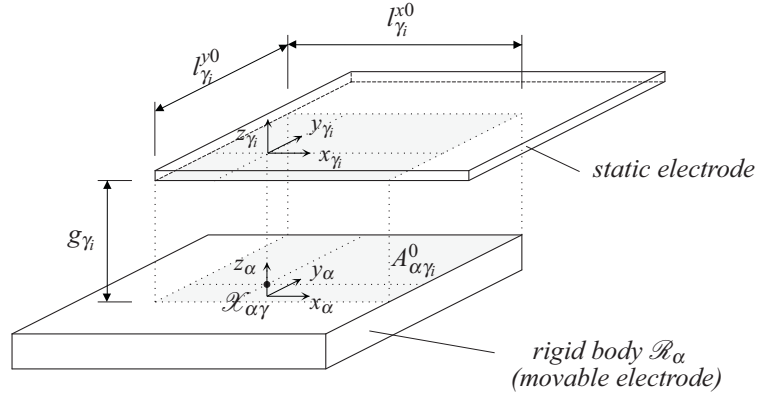


Figure 6: Capacitor in undeformed configuration

within the overlap area $A_{\alpha\gamma_i}$ in the undeformed configuration described in the coordinate system $(o_{\gamma_i}x_{\gamma_i}y_{\gamma_i}z_{\gamma_i})$ reads as

$$\hat{\mathbf{u}}_0^{\alpha\gamma_i} = \mathbf{R}_{\gamma_i}^0 \mathbf{u}_0^{\alpha\gamma_i}$$

with the rotation matrix $\mathbf{R}_{\gamma_i}^0$, describing the initial orientation of the static electrode with respect to the reference coordinate system $(o_0x_0y_0z_0)$. Hereafter, it is assumed that the electric field is ideal in the sense that stray fields are negligible, concluding that it only has one effective component normal to the static electrode. Thus, the capacity of a \mathcal{C}_{γ_i} element in the deformed configuration calculates as

$$C_{\gamma_i} = \epsilon_r \iint_{A_{\alpha\gamma_i}} \frac{1}{g_{\gamma_i}} dx_{\gamma_i} dy_{\gamma_i} \quad (13)$$

with dielectric constant ϵ_r , the overlap area $A_{\alpha\gamma_i}$ and the gap distance

$$g_{\gamma_i} = g_0 - \hat{\mathbf{u}}_0^{\alpha\gamma_i} \mathbf{e}_z,$$

with the unit vector in z_{γ_i} -direction \mathbf{e}_z . The overlap area in the deformed configuration $A_{\alpha\gamma_i}$ is given by the normal projection of the lateral edges of the static electrode on the surface of the movable electrode and thus depends on the displacements and rotations \mathbf{r}_0^α of the movable electrode \mathcal{R}_α . For the devices under consideration, however, the rotational displacement of a rigid body \mathcal{R}_α can be assumed to be small. Furthermore, the size of the overlap area $A_{\alpha\gamma_i}$ of a single \mathcal{C}_{γ_i} element is usually small in comparison to the whole overlap area of the capacitor \mathcal{C}_γ , justifying an approximation of the projected area by a rectangle, which only depends on the translational displacement vector $\hat{\mathbf{u}}_0^{\alpha\gamma_i}$. Therefore, (13) can be approximated by

$$C_{\gamma_i} \cong C_{\gamma_i}(\hat{\mathbf{u}}_0^{\alpha\gamma_i}) = \epsilon_r \frac{(L_{\gamma_i}^{x0} \pm \hat{\mathbf{u}}_0^{\alpha\gamma_i} \mathbf{e}_x) (L_{\gamma_i}^{y0} \pm \hat{\mathbf{u}}_0^{\alpha\gamma_i} \mathbf{e}_y)}{g_{\gamma_i}} \quad (14)$$

with the unit vectors \mathbf{e}_x and \mathbf{e}_y in x_{γ_i} - and y_{γ_i} -direction, respectively. Equation (14) equals a rectangular parallel plate capacitor with variable edge and gap length. The capacity of the whole capacitor \mathcal{C}_γ finally reads

$$C_\gamma \cong \sum_i C_{\gamma_i}(\hat{\mathbf{u}}_0^{\alpha\gamma_i}). \quad (15)$$

With these considerations parallel plate sense capacitors and drive comb capacitors can now be easily derived by calculating the intersection area of all rigid bodies \mathcal{R}_α and all electrodes.

3.2 ModelMEMS

The second part of the tool, *ModelMEMS*, is implemented as a library in the commercial computer algebra system *Maple*. Apart from the benefit that control engineers are familiar with computer algebra programs, the provided worksheet environment is flexible and easily expandable.

The sensor analysis in *ModelMEMS* proceeds in several steps. Firstly, the data, which is transferred from *SimMEMS* by a file format based on the eXtensible Mark-up Language (XML[14]), is read. In the next step a mathematical object is assigned to each functional object. Henceforth, one can work with these mathematical objects within the full functional range of *Maple*. This includes changing the numerical values, assigning new symbols or adding new mathematical objects to the device, which were not defined in the data file. However, during a

typical analysis, one usually proceeds by calculating the kinetic (1) and potential energies (2), (3) of the device and deriving the differential equations (5) of motion by means of the *Lagrange Formalism* (4).

The resulting equations of motion usually cover a dynamic range that is far beyond the interest of the controller design. Therefore, a modal transformation is performed allowing the user to just include the relevant dynamics of the device. To make the selection process easier all eigenmodes of the linearized mathematical model can be animated in the 3D viewer of *SimMEMS*.

At this point it is worth mentioning that, since *Maple* is used as the calculation engine, all calculation steps can be performed symbolically and/or, if desired, with arbitrary precision arithmetic. This is fundamental to prevent numerical inaccuracies and to preserve the mathematical symmetries found in these devices. Furthermore, working with symbolic or semi-symbolic equations, on the one hand, leads to a better understanding of the overall system behavior and on the other hand, keeps the possibility of choosing those parameters which shall remain symbolic and which, for the sake of simulation efficiency, shall be numeric.

For the further controller design and simulation of the closed-loop behavior in MATLAB/Simulink, a *Level 2 C-Code S-Function* simulation model can be generated from the mathematical model by the integrated code generator.

4 Conclusion

In this paper, a tool to automatically generate the mathematical model of capacitive MEMS gyroscopes in a symbolic form from geometric input data is introduced. After summarizing the advantages and disadvantages of common design strategies, a mathematical concept is presented that allows for the derivation of the equations of motion of capacitive MEMS gyroscopes by means of the well known Lagrange formalism. Therefore, the device under consideration is divided into its functional components (e.g., rigid body, beam structure, electrode). After illustrating the overall program structure, the objective of the two parts of the software are specified, followed by the introduction of several implemented algorithms.

Acknowledgments

This work was funded by the German BMBF as part of the EURIPIDES project RESTLES (project nr.: 16SV3579).

5 References

- [1] Ansys: ANSYS, Inc., <http://www.ansys.com>, 2008.
- [2] COMSOL MULTIPHYSICS: COMSOL, Inc., <http://www.comsol.com>, 2008.
- [3] CoventorWare ARCHITECT: Coventor, Inc., www.coventor.com, 2008.
- [4] Egretzberger M., Kugi A., Günthner S., Hartmann B.: *Stress measurement in a cantilevered silicon beam undergoing coupled motion of torsion and bending*. Smart Materials and Structures 16, 2007.
- [5] Günthner S.: *Entwurf und Charakterisierung von mikromechanischen Drehratensensoren in Silizium*. Aktuelle Berichte aus der Mikrosystemtechnik, Shaker Verlag, Aachen, 2006.
- [6] Han J. S., Rudnyi E. B., Korvink J. G.: *Efficient optimization of transient dynamic problems in MEMS devices using model order reduction*. Journal of Micromechanics and Microengineering, v. 15, N 4, p. 822-832, 2005.
- [7] Maple: Maplesoft a division of Waterloo Maple, Inc. Release 12.0, www.maplesoft.com, 1981-2008.
- [8] MATLAB/Simulink: The MathWorks, Inc. Release 2008b, www.mathworks.com, 1984-2007.
- [9] Pilkey W. D.: *Analysis and Design of Elastic Beams*. John Wiley & Sons, New York, 2002.
- [10] Python: Python Software Foundation. Release 2.5.2, www.python.org, 2001-2008.
- [11] Reitz S., Bastian J., Haase J., Schneider P., Schwarz P.: *System level modeling of microsystems using order reduction methods*. Analog Integrated Circuits and Signal Processing, 37, 7-16, 2003.
- [12] Rudnyi E. B., Korvink J. G.: *Model Order Reduction of MEMS for Efficient Computer Aided Design and System Simulation*. Sixteenth International Symposium on Mathematical Theory of Networks and Systems, Belgium, July 5-9, 2004.
- [13] Spong M. W., Vidyasagar M.: *Robot Dynamics and Control*. John Wiley & Sons, New York, 1989.
- [14] Extensible Markup Language: W3C, World Wide Web consortium., 1.0 (Fourth Edition), <http://www.w3.org>, 2006.